

Anisotropic spin-fluctuations in SmCoPO revealed by ^{31}P NMR measurement

Mayukh Majumder¹, K. Ghoshray^{1,*}, A. Ghoshray¹, Anand Pal², and V.P.S. Awana²

¹*ECMP Division, Saha Institute of Nuclear Physics, 1/AF Bidhannagar, Kolkata-700064, India and*

²*Quantum Phenomenon and Applications (QPA) Division,
National Physical Laboratory (CSIR), New Delhi-110012, India*

(Dated: December 9, 2011)

^{31}P NMR result in the powder sample of SmCoPO has been reported. The spectral features reveal an axially symmetric nature of the local magnetic field. At low temperature, the anisotropy of the internal magnetic field increases rapidly, with K_{ab} increasing faster than that of K_c . The dominant contribution to this anisotropy arises from Sm-4*f* electron contribution over that of Co-3*d*. The intrinsic width 2β deviates from linearity with respect to bulk susceptibility below 170 K due to the enhancement of $(1/T_2)_{\text{dynamic}}$. The significant enhancement of $(1/T_2)_{\text{dynamic}}$ along with the continuous increase of anisotropy in the internal magnetic field is responsible for the wipe out effect of the NMR signal intensity, well above T_C . Absence of anisotropy in $1/T_2$ indicates the isotropic nature of the longitudinal component of the fluctuating local magnetic field. $1/T_1$ in SmCoPO shows large anisotropy compared to that in LaCoPO. This confirms a significant contribution of Sm-4*f* electron spin fluctuations to $1/T_1$, arising from indirect RKKY type exchange interaction between Sm-4*f* moments and indicates a non-negligible hybridization between Sm-4*f* orbitals and the conduction band, over and above the itinerant character of the Co-3*d* spins. The anisotropy in $1/T_1$ originates mainly from the orientation dependence of $\chi''(\mathbf{q},\omega)$ over a contribution from H_{hf} . The 3*d*-spin fluctuations in the *ab* plane is primarily of 2D FM in nature, while along the *c*-axis, a signature of a weak 2D AFM spin fluctuations superimposed on weak FM spin-fluctuations even in a field of 7 T and far above T_N is observed. The enhancement of this AFM fluctuations of the Co-3*d* spins along *c*-axis in SmCoPO, at further low temperature is responsible to drive the system to an AFM ordered state. The interaction between Sm-4*f* and Co-3*d* spin fluctuations, should have an important role in the development of weak AFM spin fluctuations along *c*-axis.

PACS numbers: 74.70.-b, 76.60.-k

I. INTRODUCTION

The unconventional nature of the iron based (grouped in several families) superconductors has drawn immense attention from the theoreticians as well as experimentalists.¹ Presence of strongly correlated electrons are responsible for diverse electronic and magnetic properties shown by these materials. The non-superconducting parent compounds also show interesting properties^{2,3} such as spin density wave (SDW) transition, structural phase transition, itinerant ferromagnetism etc. Several members of these families show superconductivity (SC) upon carrier doping. In 1111 and 122 family, superconductivity can be achieved by Co doping in place of iron.^{4,5} It is presumed that the study of Co based non superconducting members may provide useful information about the key factor that determines the ground state i.e. either SC or magnetic.

The magnetic property of the *RECoAsO* (*RE* = rare earth) series has been investigated^{4,6-14} for both non-magnetic (La), and magnetic (Ce, Pr, Sm, Nd, and Gd) members, the *RECoPO* on the other hand has been reported for LaCoPO^{6,15-17} and CeCoPO.¹⁸ Both these compounds exhibit only ferromagnetic transition due to Co-3*d* electrons with $T_C = 35$ K and 75 K respectively. The Ce-ions are on the border to magnetism with a Kondo scale of $T_K \sim 40$ K with enhanced Sommerfield coefficient of $\gamma = 200 \text{ mJ/molK}^2$. In *RECoAsO* series, La, Ce, and Pr show paramagnetic (PM) to ferromagnetic

(FM) transition,⁸ whereas Sm, Nd, and Gd show PM \rightarrow FM \rightarrow antiferromagnetic (AFM) transition.^{8,13} The AFM transition was proposed to be mediated by the interaction between the *RE*-4*f* and the Co-3*d* electrons. Furthermore, in SmCoAsO and NdCoAsO a second AFM transition only due to *RE* ion was also reported.^{10,14} Recently it has been shown from magnetization and specific heat measurements that Sm/NdCoPO also undergo three magnetic transitions i.e. $T_{C,Co}$ (80 K), the Sm^{4*f*}-Co^{3*d*}/Nd^{4*f*}-Co^{3*d*} interplayed AFM transition (T_{N1}) below 20 K and finally Sm³⁺/Nd³⁺ spins individual AFM transitions at (T_{N2})=5.4/2.0 K.¹⁹ The important difference between these two series is that in *RECoAsO*, the T_C increases from La to Ce and remains unchanged for Pr - Gd, whereas in *LCoPO* family, the T_C increases progressively as we go down the series from La to Sm. Thus the strength of the exchange interactions changes as one replaces As by P. In both the series, the lattice volume decreases across the series. In general, with the application of chemical or physical pressure, T_C decreases due to the increment of density of state (DOS) at Fermi level (magneto-volume effect). However, due to the lattice size decrement, the three dimensionality of the magnetic interaction may enhance causing an increment of T_C , thereby confirming the active role of the competing phenomena governing the actual ground state.

Our earlier ^{31}P and ^{139}La NMR measurements in grain aligned ($c \parallel H_0$) LaCoPO (quasi 2D Fermi surface) reveal that the spin fluctuation of 3*d* electrons in PM state is ba-

sically two dimensional (2D) in nature with non negligible 3D part and it is 3D in the FM state.^{15,17} Moreover, relaxation rate shows weak anisotropy. Since SmCoPO has the minimum unit cell volume in this series, it would be interesting to study the paramagnetic state to probe the interplay between increasing interlayer interaction due to three dimensionality of the Fermi surface (causes increment of T_C) and magneto-volume effect (causes decrement of T_C). Probing dynamic spin susceptibility, the spin-lattice relaxation rate provides microscopic information on the dimensionality of spin-fluctuations. We would thus examine a few pertinent questions: (i) is the decrement of lattice volume in SmCoPO low enough to make the spin-fluctuation 3D in nature even in the paramagnetic state? (ii) Whether any anisotropy is expected in the nuclear relaxation rate in SmCoPO because the contributions of different 3d orbitals of Co and 4f orbitals of Sm to the Fermi surface, governing nuclear relaxation, would change as a result of the lattice shrinkage? and (iii) to understand the mechanism which drives the FM oriented Co-3d spins to reorder antiferromagnetically at further low temperature which persists even in a field of 14 T.

II. EXPERIMENTAL

Polycrystalline samples of SmCoPO and LaCoPO were synthesized by solid state reaction the details of which are described in Ref. 19. The powder sample was characterized using x-ray diffraction technique with CuK α radiation at room temperature in a Rigaku X-ray diffractometer. The Rietveld analysis of the X-ray powder diffraction data confirmed that the samples are crystallized in tetragonal phase with all the peaks indexed to the space group P4/nmm. The ^{31}P NMR measurements were carried out in powder samples of SmCoPO and LaCoPO, using a conventional phase-coherent spectrometer (Thamway PROT 4103MR) with a 7.0 T (H_0) superconducting magnet (Bruker). The temperature variation study was performed in an Oxford continuous flow cryostat equipped with a ITC503 controller. The spectrum was recorded by changing the frequency step by step and recording the spin echo intensity by applying a $\pi/2 - \tau - \pi/2$ solid echo pulse sequence. Shifts were measured with respect to the ^{31}P resonance line position (ν_R) in H_3PO_4 solution. The spin-lattice relaxation time (T_1) was measured using the saturation recovery method, applying a single $\pi/2$ pulse. The spin-spin relaxation time (T_2) was measured applying $\pi/2 - \tau - \pi$ pulse sequence.

III. RESULTS AND DISCUSSIONS

A. ^{31}P NMR spectra in SmCoPO

The Hamiltonian for the interaction between the nuclear and electronic spins in the presence of external field

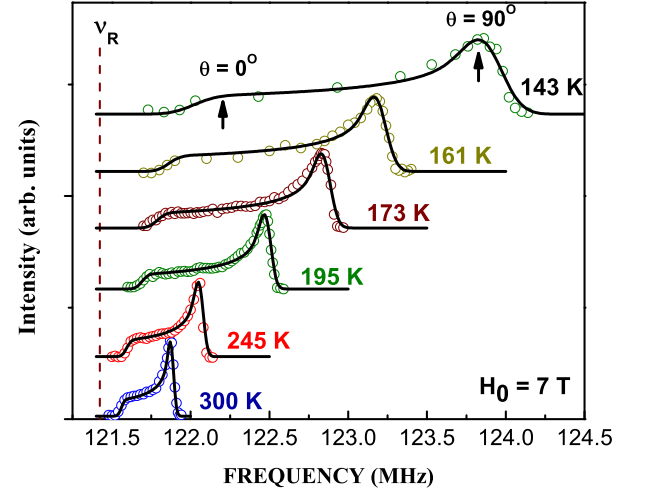


FIG. 1: (Color online) Typical ^{31}P NMR spectrum (\circ) in SmCoPO. Vertical dashed line represents reference position. Continuous lines correspond to the simulated spectrum derived from eq. 3 using Gaussian line shape. The vertical arrows indicate step ($\theta = 0^\circ$) and maximum ($\theta = 90^\circ$) respectively.

H_0 can be written as

$$H = -\gamma\hbar\mathbf{I}\cdot\mathbf{H}_0 + \sum_j \mathbf{I}\cdot\mathbf{A}_j\cdot\mathbf{S}_j + \sum_j \gamma\hbar\mathbf{I}\cdot\boldsymbol{\mu}_B g\mathbf{S}_j \frac{3\cos^2\theta_j - 1}{r_j^3}, \quad (1)$$

where the first term is the nuclear Zeeman energy, the second term represents hyperfine interaction with j th magnetic ion having spin \mathbf{S}_j and the third term denotes the dipolar interaction. In the most general case, when a nucleus experiences a completely anisotropic internal magnetic field (sum of the hyperfine and dipolar field), the resonance frequency in a single crystal is given by²⁰

$$\nu = \nu_R[1 + K_{iso} + K_{ax}(3\cos^2\theta - 1) + K_{aniso}\sin^2\theta\cos^2 2\phi], \quad (2)$$

where $K_{iso} = (K_1 + K_2 + K_3)/3$, $K_{ax} = (2K_3 - K_1 - K_2)/6$, and $K_{aniso} = (K_2 - K_1)/2$. K_1 , K_2 , and K_3 are the principal components of the total shift tensor. If a nucleus experiences an internal field of cylindrical symmetry, the third term in eq. (2) vanishes, since $K_1 \approx K_2$.

In a polycrystalline specimen, the crystallites being oriented randomly, the anisotropic shift results in a broadening proportional to the applied field. Since all values of $u = \cos\theta$ are equally probable the expression for the line shape would be $p(\nu) \sim 1/|d\nu/du|$. Superimposing a gaussian broadening of width 2β , to the resonance line from each of the crystallites, the line shape in polycrystalline sample will be

$$I(\nu') = \int_{-\infty}^{\infty} p(\nu) \exp[-(\nu - \nu')^2/2\beta^2] d\nu. \quad (3)$$

The shift parameters K_{iso} , K_{ax} and linewidth (2β) can be obtained by fitting the spectra using eq. (3).

Figure 1 shows some typical ^{31}P NMR spectra in polycrystalline SmCoPO at different temperatures. The resonance line shape corresponds to a powder pattern for a spin $I = 1/2$ nucleus experiencing an axially symmetric local magnetic field, as expected for SmCoPO having tetragonal symmetry. The step in the low-frequency side corresponds to $H_0 \parallel c$ ($\theta = 0^\circ$) and the maximum in high frequency side corresponds to $H_0 \perp c$ ($\theta = 90^\circ$). The shift of the step with respect to the reference position (ν_R), corresponds to K_c and that of the maximum corresponds to K_{ab} , where $K_{iso} = \frac{2}{3}K_{ab} + \frac{1}{3}K_c$ and $K_{ax} = \frac{1}{3}(K_c - K_{ab})$. The continuous line superimposed on each experimental line is the calculated spectrum corresponding to eq. 3 using Gaussian line shape. Most important feature is that the separation between the step, K_c and the maximum, K_{ab} increases at low temperature along with line broadening. In particular, K_{ab} shows much larger change than that of K_c . Finally, the resonance line could not be detected below 130 K, (T_C at $H=7$ T is about 110 K as determined from the derivative of the χ versus T curve; not shown here). The line did not reappear till the lowest temperature. Such thing did not happen in case of ^{31}P and ^{139}La NMR studies in LaCoPO, where the resonance line was detected¹⁷ even below T_C .

1. ^{31}P NMR wipe out and spin-spin relaxation rate $1/T_2$

Figure 2 shows the variation of 2β with the bulk magnetic susceptibility, χ (with temperature as implicit parameter) in SmCoPO, depicting a linear χ dependence of 2β in the range 173-300 K. This arises mainly from the contribution due to the demagnetizing field. Below this range there is a significant deviation from linearity, showing a large enhancement. To get a more quantitative picture, ^{31}P spin-spin relaxation time (T_2) also known as the transverse relaxation time was measured, as a function of temperature (inset (b) of Fig. 2). In this measurement, the echo integral (which arises from the transverse magnetization) was taken as a function of time delays (τ) between two rf pulses. The recovery of the transverse magnetization was found to be exponential at all temperatures. T_2 was obtained by fitting the equation $M(2\tau) = M_0 \exp(-2\tau/T_2)$, (solid lines in the inset (a) in Figure 2.) where M_0 is the initial magnetization. At any temperature, the magnitude of T_2 remains same when measured at the position of the maximum ($\theta = 90^\circ$) and at the step ($\theta = 0^\circ$) respectively, indicating its isotropic nature.

In general, $1/T_2$ can be written as the sum of the contribution from (i) dipolar interaction between the nuclear magnetic moments which is temperature and field independent ($1/T_2|_{static}$) and (ii) the dipolar and hyperfine interactions of the nuclei with the longitudinal component of the fluctuating magnetic field produced by the neighboring Co^{2+} 3d-spins and Sm 4f-spins. This dynamic part $1/T_2|_{dynamic}$, is temperature

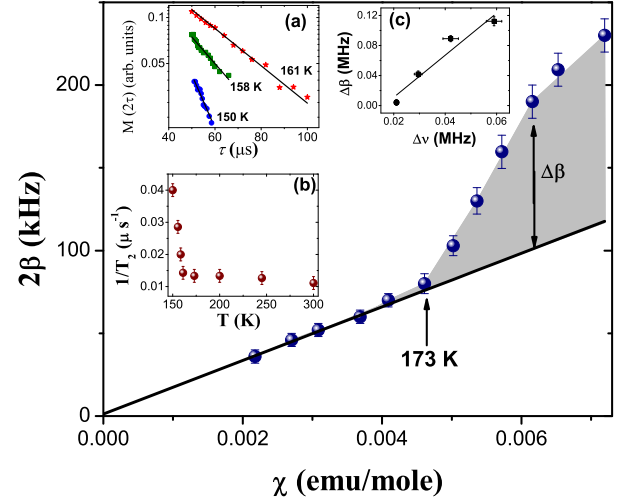


FIG. 2: (Color online) The variation of 2β against magnetic susceptibility (solid circle) in SmCoPO, solid line is the linear fit. Inset (a): recovery of transverse magnetization at different temperatures, solid lines corresponds to $M(2\tau) = M_0 \exp(-2\tau/T_2)$; (b) $1/T_2$ (μs^{-1}) versus temperature; (c): $\Delta\nu$ (MHz) versus $\Delta\beta$ (MHz), solid line is the linear fit as discussed in the text.

dependent, when the fluctuation frequency becomes close to nuclear resonance frequency below a certain temperature, due to the development of short range correlation among the electronic spins as T_C is approached. In weak collision fast motion approximation, one can express $1/T_2|_{dynamic}$, in terms of the spectral density of the spin-fluctuating hyperfine field at zero frequency,^{21,22}

$$1/T_2|_{dynamic} = \gamma_n^2 < \delta H_z^2 > \tau(T) + 1/2T_1 \quad (4)$$

where δH_z is the local longitudinal field originating from a magnetic moment sitting at a distance r apart from the probed nuclear spin, and τ stands for correlation time, which is only determined by the dynamics of the exchanged coupled magnetic ions. Therefore, the observed θ independent behavior of T_2 , as mentioned above indicates that the longitudinal component of the fluctuating electronic magnetic field at the ^{31}P nuclear site is isotropic in nature. It is to be noted that the intrinsic width, 2β in Eq. 3 contains sum of the contributions from $1/T_2|_{static}$, $1/T_2|_{dynamic}$ and that due to the demagnetizing field. Among them the first contribution is magnetic field independent while the second and third depend on field and the magnetic susceptibility.²³

The contribution $2\beta_{dynamic}$ to the total 2β was estimated, by subtracting the contribution due to the linear part determined from the extrapolated values (larger χ_M values in Fig. 2) from 2β . In the inset (c) of Fig. 2, we have plotted this $2\beta_{dynamic}$ denoted as $\Delta\beta$ versus the line width ($\Delta\nu$) obtained from the measured T_2 . The linear behavior confirms that the observed large enhancement of 2β below 173 K arises due to the enhancement of $1/T_2$ or more specifically $(1/T_2)_{dynamic}$. As T_2 reaches a value

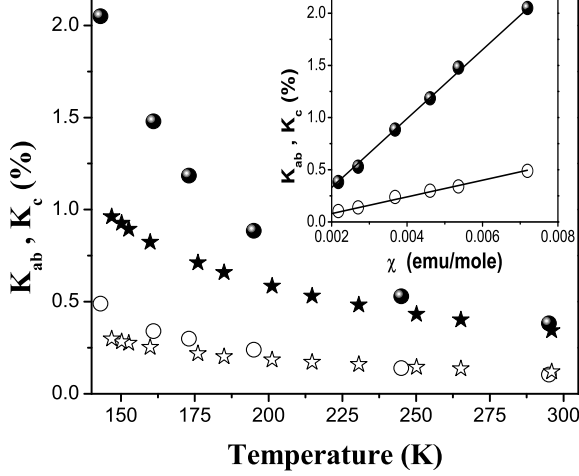


FIG. 3: K_{ab} , K_c vs temperature for SmCoPO (filled circle and open circle respectively) and K_{ab} , K_c vs temperature for LaCoPO (filled star and open star respectively), Inset shows K_{ab} , K_c vs χ for SmCoPO and the solid line is the linear fit.

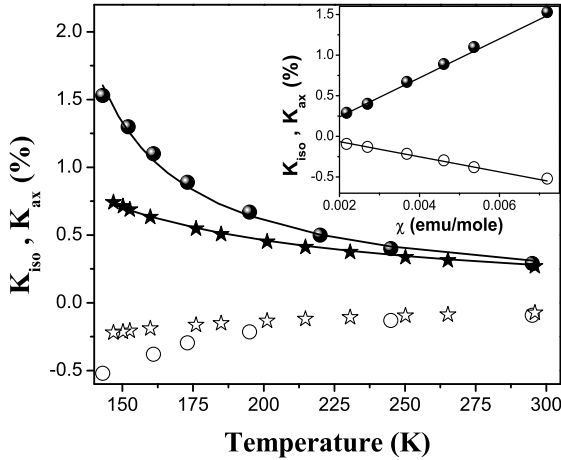


FIG. 4: K_{iso} , K_{ax} vs temperature for SmCoPO (filled circle and open circle respectively) and K_{iso} , K_{ax} vs temperature for LaCoPO (filled star and open star respectively), solid lines correspond to Eq. 6. Inset shows K_{iso} , K_{ax} vs χ for SmCoPO and the solid line is the linear fit.

of 25 μ s at 150 K, there is a possibility that at lower temperature, it becomes so short that one has to apply a delay time τ between the two rf pulses ($\pi/2 - \tau - \pi/2$) used to observe the spin echo, which is comparable to or shorter than the dead time of the spectrometer. As a consequence, the NMR signal coming from the ^{31}P nuclei can not be digitized by the spectrometer, resulting the whole signal to vanish.

B. Knight shift and hyperfine field

Figures 3 and 4 show temperature dependence of shift parameters K_c , K_{ab} , K_{iso} and K_{ax} in SmCoPO and the same in LaCoPO for comparison. Around 300 K, shift parameters for LaCoPO and SmCoPO are of same magnitude, however, at low temperature, K_{ab} , K_c , K_{iso} and K_{ax} for SmCoPO increases rapidly than in LaCoPO. Measured shift can be written as $K = K_0 + K(T)$, where K_0 is the temperature independent contribution arising from conduction electron spin susceptibility, orbital susceptibility and diamagnetic susceptibility of core electrons. $K(T)$ arises from the temperature dependent susceptibility due to Co-3d and Sm-4f spins,

$$K(T) = (H_{hf}/N\mu_B)\chi(T) \quad (5)$$

H_{hf} is the total coupling constant due to the electron nuclear hyperfine and dipolar interactions, N is the avo-gadro number and μ_B is the Bohr magneton. Insets of Figs. 3 and 4 show linear variation of K_c , K_{ab} , K_{iso} and K_{ax} with $\chi = M/H$. From these plots the obtained values of the coupling constants are H_{hf}^{ab} , H_{hf}^c , H_{hf}^{iso} , H_{hf}^{ax} are 18.4, -4.46, 13.4 and -5.19 kOe/ μ_B respectively. Using the atomic coordinates of Sm, Co and P, H_{dip}^{ax} (-0.44 kOe/ μ_B) at the ^{31}P site was calculated from Eq. 9 of sec.III.C. The value is one order of magnitude smaller than that of experimental H_{hf}^{ax} . Thus the observed temperature dependent anisotropic part of the shift is mainly due to the hyperfine interaction. If we consider that the contribution to K_{ax} due to Co-3d electrons is nearly same in LaCoPO and SmCoPO, then the observed larger enhancement of K_{ax} in SmCoPO at low temperature compared to that in LaCoPO (Fig. 4) is a signature of more pronounced contribution of Sm-4f electrons over that of Co-3d for producing anisotropic local magnetic field at the ^{31}P site.

Temperature dependence of K_{iso} can be well described by the Curie-Weiss type behavior,

$$K_{iso}(T) = (H_{hf}^{iso}/N\mu_B) \frac{C}{(T - \theta)} \quad (6)$$

as represented by the continuous line in figure 4 for La-CoPO and SmCoPO. The estimated P_{eff} value from Curie-Weiss constant (C) are $1.4\mu_B$ with $\theta=53$ K for La-CoPO and $1.65\mu_B$ with $\theta=110$ K for SmCoPO, which are in close agreement with those determined from magnetic susceptibility data.¹⁹ This indicates that there is a contribution of Sm 4f moment over that of Co 3d moment even in the paramagnetic state. It is to be noted that in NdFeAsO $_{1-x}$ F $_x$ and CeCoAsO the ^{75}As Knight shift^{24,25} was found to be influenced by 4f moments though As is situated in a different plane. A notable difference between FeAs based systems and CoP/CoAs based systems is that the hyperfine field at the ^{75}As site in LaFeAsO $_{(1-x)}$ F $_x$ is temperature independent and the temperature dependence appears only when La is replaced by other rare earths.^{24,26} Whereas, in CoP/CoAs

based systems, the hyperfine field is temperature dependent even in $\text{LaCoPO}^{15,16}$ and LaCoAsO^{12} . Substitution of other rare earth gives an additional temperature dependent contribution to the shift arising from $4f$ electrons superimposed on that due to Co $3d$ electrons.

C. Nuclear spin-lattice relaxation rate $1/T_1$

$1/T_1$ was determined from the recovery of the longitudinal component of the nuclear magnetization $M(\tau)$ as a function of the delay time τ using equation

$$M(\tau) = M(\infty)(1 - \exp^{-\tau/T_1}) \quad (7)$$

for nuclear spin $I=1/2$. The recovery curves (inset (a) of Fig. 5) were found to be exponential throughout the whole temperature range, as expected for an ensemble of $I=1/2$ nuclei with a common spin temperature. This confirms good sample homogeneity with negligible amount of phosphorous containing impurity phase. The temperature dependence of the ^{31}P nuclear spin-lattice relaxation rates $(1/T_1)_{ab}$ and $(1/T_1)_c$ in SmCoPO (inset(b) of Fig. 5) in the temperature range 140 - 300 K clearly show the anisotropic nature. The T_1 values in SmCoPO are one order of magnitude shorter than that in LaCoPO near 300 K and becomes two orders of magnitude shorter near 140 K. In case of $\text{SmFeAsO}_{1-x}\text{F}_x$ ^{19}F NMR²⁶ relaxation rate $(1/T_1)$ was three orders of magnitude higher than that in $\text{LaFeAsO}_{1-x}\text{F}_x$.²⁷ This enhancement in $1/T_1$ was also observed in case of ^{75}As $1/T_1$ in 1111 superconductor with Pr and Nd as rare earth element.²⁸ The enhancement in $1/T_1$ was assigned due to the $4f$ electrons and not due to the Fe $3d$ electrons. Prando et al.²⁶ have concluded that the increment of $1/T_1$ from 200 K in $\text{SmFeAsO}_{1-x}\text{F}_x$ was due to the Sm $4f$ electrons via the indirect RKKY exchange coupling and which indicates that there is a non-negligible hybridization between Sm $4f$ with conduction electrons i.e. the $4f$ electrons are not fully localized in nature. In SmCoPO the large enhancement in magnitude of $1/T_1$ at low temperature with respect to that in LaCoPO should also arise due to the contribution of Sm $4f$ electrons through the magnetic dipolar interaction and the hyperfine interaction (through RKKY type conduction electron mediated $c-f$ exchange) over the contribution of Co $3d$ electrons (which is also present in LaCoPO). Moreover, the continuous enhancement of $1/T_1$ in SmCoPO from below 300 K, indicates the signature of the development of short range correlation far above T_C . This should be characteristic of itinerant magnetism of both Co $3d$ and Sm $4f$ electrons.²⁹ So ^{31}P will feel the effect of itinerant Co $3d$ via the hybridization between Co $3d$ and P $2p$ and also feel the effect of Sm $4f$ electrons via RKKY interaction through the conduction electrons along with the magnetic dipolar interaction with the same.

Contribution to spin-lattice relaxation rate due to $4f$

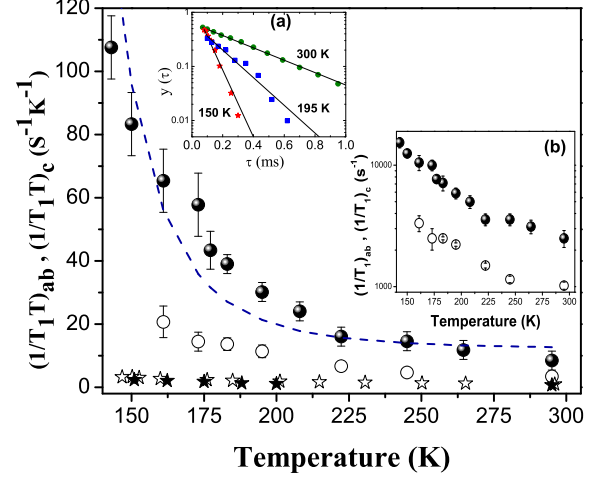


FIG. 5: $(1/T_1 T)_{ab}$ (filled circle), $(1/T_1 T)_c$ (open circle) versus T for SmCoPO and $(1/T_1 T)_{ab}$ (filled star), $(1/T_1 T)_c$ (open star) versus T for LaCoPO . The dashed line corresponds to Eq. 16. Inset(a): recovery curves at different temperatures where $y(\tau) = \frac{M(\infty) - M(\tau)}{M(\infty)}$ and Inset (b): $(1/T_1)_{ab}$ (filled circle) and $(1/T_1)_c$ (open circle) vs T for SmCoPO .

spin fluctuation (from Sm) via the dipolar coupling³⁰ is

$$(1/T_1)_{\text{dip}} = \frac{\sqrt{2\pi}\gamma_n^2(g\mu_B)^2}{6\omega_e} J(J+1) \sum_i r_i^{-6} \times [F_i(\alpha_i, \beta_i, \gamma_i) + F'_i(\alpha_i, \beta_i, \gamma_i)], \quad (8)$$

where $F_i(\alpha_i, \beta_i, \gamma_i)$ and $F'_i(\alpha_i, \beta_i, \gamma_i)$ are geometrical factors which depend on $\alpha_i, \beta_i, \gamma_i$, the direction cosines of r_i connecting the i -th Sm atom and ^{31}P nuclear spin with respect to the principal axes of the dipolar field tensor. Using the structural parameters¹⁹ for SmCoPO we have calculated the dipolar field at the ^{31}P nuclear site arising from Sm moment with the formula,

$$H_{\text{dip}} = \mu \sum \frac{(3r_j r_k - r^2 \delta_{jk})}{r^5}; j, k = x, y, z \quad (9)$$

μ is the magnetic moment of Sm moment. The direction of the principal components of the dipolar tensor coincide with the crystallographic axes system and this makes calculation of $F_i(\alpha_i, \beta_i, \gamma_i)$ and $F'_i(\alpha_i, \beta_i, \gamma_i)$ simple. Thus the lattice sum of eq. 8

$$\sum_i r_i^{-6} [F_i(\alpha_i, \beta_i, \gamma_i) + F'_i(\alpha_i, \beta_i, \gamma_i)] = 2.143 \times 10^{46} \text{ cm}^{-6}.$$

The electronic exchange frequency ω_e is estimated from the Neel temperature ($T_N = 5.4$ K) of the Sm- $4f$ moment¹⁹ by

$$(\hbar\omega_e)^2 = \frac{1}{6z} \frac{(3k_B T_N)^2}{J(J+1)}. \quad (10)$$

Taking $z=4$, number of the nearest neighbor Sm spins $\omega_e = 1.46 \times 10^{11} \text{ sec}^{-1}$. Finally, $(1/T_1)_{\text{dip}} = 434 \text{ sec}^{-1}$. At

300 K the average value of $1/T_1$ in SmCoPO for $\theta=0$ and $\theta=\pi/2$ is $\sim 1760 \text{ sec}^{-1}$. The value of $1/T_1$ at 300 K in LaCoPO is $\sim 300 \text{ sec}^{-1}$. If we now assume that the contribution due to Co-3d spins is nearly same in LaCoPO and SmCoPO, then also $[(1/T_1)_{\text{SmCoPO}} - (1/T_1)_{\text{LaCoPO}}]$ is more than three times larger than $(1/T_1)_{\text{dip}}$ for Sm 4f spins i.e. the main contribution to $1/T_1$ in SmCoPO comes from hyperfine interaction with the Sm-4f spins.

Main panel of Fig. 5 shows the $(1/T_1 T)_{ab}$ and $(1/T_1 T)_c$ vs T curves in SmCoPO and in LaCoPO. In SmCoPO $(1/T_1 T)_{ab}$ increases much faster than that of $(1/T_1 T)_c$. Whereas, in LaCoPO this anisotropy is negligible. This enhanced anisotropy is a signature of contribution of anisotropic Sm 4f orbitals along with the Co 3d orbitals. In general, $(1/T_1 T)_{SF}$ is given by

$$(1/T_1 T)_{SF} \propto \sum_q |H_{hf}(q)|^2 \chi''(q, \omega_n) / \omega_n \quad (11)$$

where $\chi''(q, \omega_n)$ is the imaginary part of the transverse dynamical electron spin susceptibility, γ_n and ω_n are the nuclear gyromagnetic ratio and Larmor frequency respectively. $H_{hf}(q)$ is the hyperfine form factor. Terasaki³¹ et al. in LaFeAsO_{0.7} and Kitagawa³² et. al. in BaFe₂As₂ had shown that at P site $H_{hf}(q)$ is non-zero for $q = 0$ and also non-zero for $q \neq 0$ (inplane off-diagonal pseudo-dipolar hyperfine field has a non zero value along c axis for $q = (\pm\pi, \pm\pi)$). $q \neq 0$ contribution have been found at As site for BaFe₂As₂,³² SrFe₂As₂,³³ LaFeAsO, LaFeAsO_{1-x}F_x³⁴ and also in Co doped BaFe₂As₂³⁴⁻³⁶ systems. This indicates that $1/T_1 T$ at P site can feel ferromagnetic spin-fluctuations as well as antiferromagnetic spin-fluctuations.

The directional dependence in $(1/T_1 T)_{ab}$ and $(1/T_1 T)_c$ can be due to anisotropy in H_{hf} or due to anisotropy of $\chi''(q, \omega_n)$, or both. Inset of Fig. 6 shows that the ratio $(1/T_1 T)_{ab}/(1/T_1 T)_c$ is higher than that of the ratio $[(H_{hf}^{ab})^2 + (H_{hf}^c)^2]/2(H_{hf}^{ab})^2$, which suggests that there is also a significant anisotropy in $\chi''(q, \omega_n)$. $(1/T_1 T)_c$ and $(1/T_1 T)_{ab}$ are related to χ''_{in} (in plane) and χ''_{out} (out of plane) by the following relations,³⁷

$$(1/T_1 T)_c \propto \sum_q 2|H_q^{in}|^2 \frac{\chi''_{in}(q, \omega)}{\omega_n}, \quad (12)$$

$$(1/T_1 T)_{ab} \propto \sum_q [|H_q^{out}|^2 \frac{\chi''_{out}(q, \omega)}{\omega_n} + |H_q^{in}|^2 \frac{\chi''_{in}(q, \omega)}{\omega_n}], \quad (13)$$

Using these relations, we have estimated χ''_{in}/ω_n and χ''_{out}/ω_n , whose T dependence are shown in Fig. 6. χ''_{out}/ω_n is about two orders of magnitude higher than χ''_{in}/ω_n . Such anisotropy in relaxation rate was also observed in other FeAs based systems like BaFe₂As₂,³² SrFe₂As₂,³³ LaFeAsO, LaFeAsO_{1-x}F_x³⁴ and also Co doped BaFe₂As₂³⁴⁻³⁶ systems. Define $\mathbf{A} = [(1/T_1 T)_{ab}/(1/T_1 T)_c]/[(H_{hf}^{ab})^2 + (H_{hf}^c)^2]/2(H_{hf}^{ab})^2$. \mathbf{A} will be one if there is no anisotropy in χ''/ω_n and \mathbf{A}

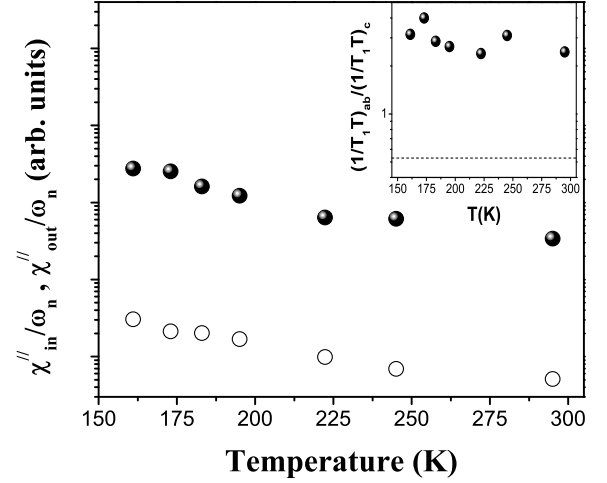


FIG. 6: Variation of χ''_{in}/ω_n (open circle) and χ''_{out}/ω_n (filled circle) with respect to T for SmCoPO. Inset: $(1/T_1 T)_{ab}/(1/T_1 T)_c$ versus T and the dashed line indicates the value of $[(H_{hf}^{ab})^2 + (H_{hf}^c)^2]/2(H_{hf}^{ab})^2 \approx 0.53$.

will deviate from unity if anisotropy comes from χ''/ω_n . The values of \mathbf{A} obtained using the reported ⁷⁵As NMR T_1 data in BaFe₂As₂, SrFe₂As₂, and LaFeAsO are 2.4, 1.75, 1.5 respectively. Also in Co doped BaFe₂As₂, $(1/T_1 T)_{ab}/(1/T_1 T)_c$ is between 1-2. The value of \mathbf{A} in case of SmCoPO is 5.66. This clearly indicates a dominant contribution of Sm 4f spin fluctuations over that due to Co-3d electrons, in the anisotropy of $1/T_1$ in SmCoPO. Anisotropy in spin-fluctuations arises from the spin-orbit coupling for which the spin and orbital degrees of freedom get mixed and dynamic magnetic susceptibility becomes anisotropic. So the preferred directions of orbital fluctuations are determined by the geometry and orbital characters of the Fermi surfaces. Band structure calculations using tight-binding approximation is highly needed to evaluate which 3d and 4f orbital fluctuations are responsible for anisotropy in spin-fluctuations in SmCoPO.

When the Knight shift and nuclear spin-lattice relaxation process are governed by conduction electrons, $1/T_1 T K^2$ is constant. If there is an exchange interaction between the electrons then using Stoner approximation along with random phase approximation, modified Korringa relation can be written as³⁸⁻⁴⁰ $S_0/T_1 T K_{spin}^2 = K(\alpha)$, where $S_0 = (\hbar/4\pi k_B)(\gamma_e/\gamma_n)^2$ and

$$K(\alpha) = \langle (1 - \alpha_0)^2 / (1 - \alpha_q)^2 \rangle_{FS}. \quad (14)$$

$\alpha_q = \alpha_0 \chi_0(q)/\chi(0)$ is the q -dependent susceptibility enhancement, with $\alpha_0 = 1 - \chi_0(0)/\chi(0)$ representing the $q = 0$ value. The symbol $\langle \rangle_{FS}$ means the average over q space on the Fermi surface. $\chi(0)$ and $\chi_0(q)$ represents the static susceptibility and the q mode of the generalized susceptibility of noninteracting electrons respectively. $K(\alpha) < 1$ means the spin-fluctuations are enhanced around $q = 0$, leading to the predominance of fer-

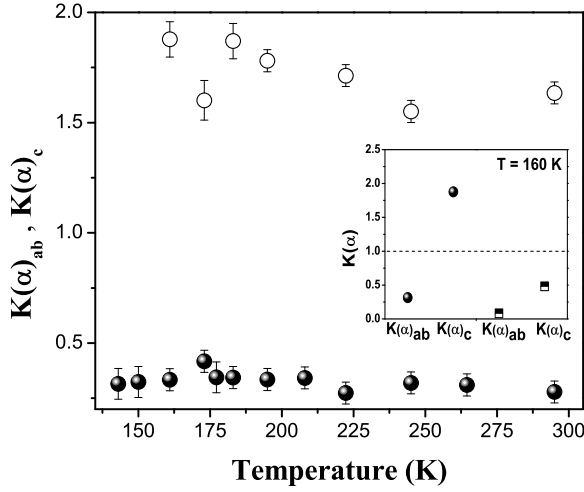


FIG. 7: $K(\alpha)_{ab}$ (filled circle) and $K(\alpha)_c$ (open circle) versus T for SmCoPO. Inset shows $K(\alpha)_{ab}$, $K(\alpha)_c$ (filled circle) for SmCoPO and $K(\alpha)_{ab}$, $K(\alpha)_c$ (half-filled square) for LaCoPO at 160 K and the dashed line corresponds to $K(\alpha) = 1$.

romagnetic correlations and $K(\alpha) > 1$ signifies that spin-fluctuations are enhanced away from $q = 0$. This would indicate a tendency towards AF ordering (at $q \neq 0$). Inset of Fig. 7. shows that for LaCoPO, $K(\alpha)_{ab}$ and $K(\alpha)_c$ are < 1 when calculated at 160 K, which shows the predominance of ferromagnetic spin-fluctuations in both these directions. Whereas, in SmCoPO, $K(\alpha)_{ab} < 1$ but $K(\alpha)_c > 1/(1.8)$, calculated at 160 K. The values of $K(\alpha)_{ab}$, $K(\alpha)_c$ for LaCoPO and the value $K(\alpha)_{ab}$ for SmCoPO suggest that the spin fluctuations are ferromagnetic in nature both in the ab -plane and along the c direction in LaCoPO. However, the same in SmCoPO is FM in the ab -plane, while along c -direction there is a signature of the presence of $q \neq 0$ modes in addition to $q = 0$ modes. Thus in SmCoPO their exist weak AFM spin-fluctuations along c axis in contrast to LaCoPO (inset of Fig. 7).

According to the theory of weak itinerant ferromagnet, if 3D/2D spin-fluctuations are dominant^{41,42} then $1/T_1T \propto \chi^{1(3/2)}$. Fig. 8 shows the T versus $(1/T_1TK)_{ab}$ and $(1/T_1TK^{3/2})_{ab}$ plots revealing dominant 2D FM spin-fluctuations in the ab plane of SmCoPO particularly in the paramagnetic region.

1. Spin fluctuations parameters

Following the theory of Ishigaki and Moriya⁴² one can write the imaginary part of dynamic spin susceptibility in terms of the two spin-fluctuation parameters T_0 and T_A which characterize the width of the spin excitations spectrum in frequency and wave vector (\mathbf{q}) space respectively. For ferromagnetic correlations, we have

$$\chi(\mathbf{q}, \omega) = \frac{\pi T_0}{\alpha_Q T_A} \left(\frac{x}{k_B 2\pi T_0 x(y + x^2) - i\omega\hbar} \right), \quad (15)$$

where $x = \mathbf{q}/q_B$ with q_B being the effective zone boundary vector, α_Q a dimensionless interaction constant close to unity for a strongly correlated system, $y = 1/2\alpha_Q k_B T_A \chi(0,0)$. Here the susceptibility is per spin and in units of $4\mu_B^2$ and has the dimension of inverse of energy, T_0 and T_A are in Kelvin. From Eq. 11 one can derive $\chi''(\mathbf{q}, \omega_n)$ in the limit $\omega_n \rightarrow 0$, since $\hbar\omega_n \ll k_B T$. For 3D spin fluctuations governing the relaxation process, one has to integrate $\chi''(\mathbf{q}, \omega_n)/\omega_n$, over a sphere of radius $\mathbf{q}_B (6\pi^2/v_0)^{1/3}$, whereas, in case of 2D spin fluctuations, the integration has to be done over a disc of radius $\mathbf{q}_B (4\pi/v_0)^{1/2}$. v_0 corresponds to the atomic volume of Co. So in the latter case

$$1/T_1T = \gamma_n^2 H_{hf}^2 / 4T_A T_0 y^{3/2} + \alpha \quad (16)$$

where according to 2D SCR theory, y can be approximately written as $y = (T/6T_0)^{2/3} \exp(-p^2 T_A/10T)$, where p is the ferromagnetic moment in μ_B units and α is the temperature independent contribution of $1/T_1T$ arising from the orbital moment of p and d electrons and the spin of the conduction electrons. Using Eq. 16, we have estimated the spin-fluctuation parameters T_A and T_0 in SmCoPO as 21000 and 2043 K respectively. The dashed line of Fig. 5 corresponds to Eq. 16.

2. Spin fluctuations and possible antiferromagnetic spin-structure

According to the SCR theory of itinerant antiferromagnetism if 3D(2D) spin-fluctuations governs the relaxation process⁴² then $1/T_1T$ is proportional to $\chi^{1/2, (1)}$. Inset of Fig. 8 shows that $(1/T_1T)_c$ is nearly proportional to the intrinsic spin susceptibility, probed by NMR shift K_c (which is proportional to χ_c), which reveals that AFM spin-fluctuations are also nearly 2D in nature. A small slope in this plot could be a signature of the presence of weak FM spin fluctuations superimposed on the weak 2D AFM one along the c -direction. Presence of FM spin fluctuation along c -direction due to the inter layer exchange interaction, in the paramagnetic phase in SmCoPO is relevant (observed from ¹³⁹La NMR in LaCoPO as shown in Ref. 17) as the FM transition precedes the AFM transition. Possibly this is the reason for which $\chi''_{in}/\omega_n < \chi''_{out}/\omega_n$, because χ''_{out}/ω_n arises from the sum of the contributions from $q = 0$ and $q \neq 0$ mode of spin-fluctuations. The appearance of weak AFM spin-fluctuations of the Co-3d spins, along c -direction, far above the ferromagnetic transition (which was absent in case of LaCoPO) is a signature of AF exchange interaction between the Sm-4f and the Co-3d electrons. This is consistent with the fact that Sm-O plane is situated in between two Co-P planes and both are parallel to ab plane. Due to the presence of AF interaction along c -direction, though the Co spins in each Co-P plane order ferromagnetically below T_C , at lower temperature when the AF exchange interaction between the Sm-4f and Co-3d spins, along the c -direction becomes more stronger,

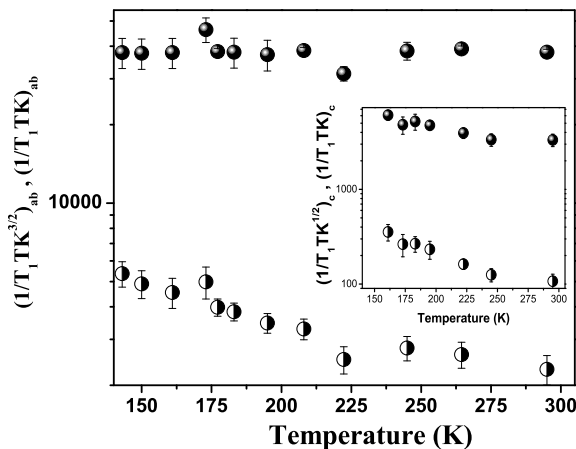


FIG. 8: $(1/T_1 TK^{3/2})_{ab}$ (filled circle), $(1/T_1 TK)_{ab}$ (half-filled circle) versus T for SmCoPO and inset shows $(1/T_1 TK^{1/2})_c$ (half-filled circle), $(1/T_1 TK)_c$ (filled circle) versus T for SmCoPO

the Co-3d spins in the two adjacent planes would try to align antiparallel even if they remain parallel to each other within a plane. As a result, the system orders antiferromagnetically. Such type of spin structure in NdCoAsO has recently been proposed from elastic neutron scattering study.¹⁰ Signature of the presence of weak AF exchange interaction between the Sm-4*f* and Co-3d spins even above T_C obtained from ^{31}P spin-lattice relaxation data, could possibly be the reason for the persistence of AF transition in SmCoPO even in a magnetic field of 14 T, whereas, it disappears completely at $H=5$ T in NdCoPO, though the Nd 4*f* effective moment is higher than that of Sm 4*f*. As the lattice parameter c in SmCoPO is less than that in NdCoPO, therefore, the strength of the AF exchange interaction between Sm-4*f* and Co-3d spins present along the c -direction could be more stronger in SmCoPO than in NdCoPO. Therefore, the ^{31}P NMR shift and the spin-lattice relaxation studies in other mem-

bers of LCoPO series would be interesting to understand the effect of the change in the lattice volume, on the nature of the spin fluctuations and as well as the extent of anisotropy, which drives the system to a particular ground state.

IV. CONCLUSIONS

We have reported ^{31}P NMR results in the powder sample of SmCoPO. The spectral features reveal an axially symmetric nature of the local magnetic field. At low temperature, the anisotropy of the internal magnetic field increases, with K_{ab} increasing faster than that of K_c . The intrinsic width 2β shows a linear variation with χ_M in the range 300 - 170 K. Deviation from linearity below 170 K arises due to the enhancement of $(1/T_2)_{dynamic}$. This enhancement of $(1/T_2)_{dynamic}$ along with the continuous increase of anisotropy in the internal magnetic field is responsible for the wipe out of the NMR signal, well above T_C . Absence of anisotropy in $1/T_2$ indicates the isotropic nature of the longitudinal component of the fluctuating local magnetic field.

Observed large anisotropy in $1/T_1$ of SmCoPO compared to that of LaCoPO, confirms a significant contribution of Sm-4*f* electron arising from indirect RKKY interaction. This indicates a non-negligible hybridization between Sm-4*f* orbitals and the conduction band, over and above the itinerant character of the Co-3d spins. The anisotropy of $1/T_1$ originates mainly from the orientation dependence of $\chi''(\mathbf{q},\omega)$. The 3d-spin fluctuations in the ab plane is primarily of 2D FM in nature similar to that in LaCoPO, while along the c -axis, a signature of weak 2D AFM spin-fluctuations superimposed on weak FM spin-fluctuations even in a field of 7 T and far above T_C is observed. The enhancement of this AFM exchange interaction below T_C should be responsible to drive the Co moment to an AFM ordered state.

* Electronic address: kajal.ghoshray@saha.ac.in

¹ D. C. Johnston, *Advances in Physics* **59**, 803 (2010), and references therein.

² Michael A. McGuire, Andrew D. Christianson, Athena S. Sefat, Brian C. Sales, Mark D. Lumsden, Rongying Jin, E. Andrew Payzant, David Mandrus, Yanbing Luan, Veerle Keppens, Vijayalakshmi Varadarajan, Joseph W. Brill, Raphael P. Hermann, Moulay T. Sougrati, Fernande Grandjean, and Gary J. Long, *Phys. Rev. B* **78**, 094517 (2008).

³ Ying Chen, J. W. Lynn, J. Li, G. Li, G. F. Chen, J. L. Luo, N. L. Wang, Pengcheng Dai, C. dela Cruz, and H. A. Mook, *Phys. Rev. B* **78**, 064515 (2008).

⁴ Athena S. Sefat, Ashfia Huq, Michael A. McGuire, Rongying Jin, Brian C. Sales, David Mandrus, Lachlan M. D. Cranswick, Peter W. Stephens, and Kevin H. Stone, *Phys. Rev. B* **78**, 104505 (2008).

⁵ Athena S. Sefat, Rongying Jin, Michael A. McGuire, Brian C. Sales, David J. Singh, and David Mandrus, *Phys. Rev. Lett.* **101**, 117004 (2008).

⁶ Hiroshi Yanagi, Ryuto Kawamura, Toshio Kamiya, Yoichi Kamihara, Masahiro Hirano, Tetsuya Nakamura, Hitoshi Osawa, and Hideo Hosono, *Phys. Rev. B* **77**, 224431 (2008).

⁷ H. Ohta and K. Yoshimura, *Phys. Rev. B* **79**, 184407 (2009).

⁸ H. Ohta and K. Yoshimura, *Phys. Rev. B* **80**, 184409 (2009).

⁹ Andrea Marcinkova, David A. M. Grist, Irene Margiolaki, Thomas C. Hansen, Serena Margadonna, and Jan-Willem G. Bos, *Phys. Rev. B* **81**, 064511 (2010).

¹⁰ Michael A. McGuire, Delphine J. Gout, V. Ovidiu Garlea, Athena S. Sefat, Brian C. Sales, and David Mandrus, Jr., *Phys. Rev. B* **81**, 104405 (2010).

- ¹¹ H. Ohta, C. Michioka, and K. Yoshimura, J. Phys. Soc. Jpn. **79**, 054703, (2010).
- ¹² Hiroto Ohta, Chishiro Michioka, Akira Matsuo, Koichi Kindo, and Kazuyoshi Yoshimura, Phys. Rev. B **82**, 054421 (2010).
- ¹³ V. P. S. Awana, I. Nowik, Anand Pal, K. Yamaura, E. Takayama-Muromachi, and I. Felner, Phys. Rev. B **81**, 212501 (2010).
- ¹⁴ A. Pal, M. Tropeano, S. D. Kaushik, M. Hussain, H. Kishan, V. P. S. Awana, J. Appl. Phys **109**, 07E121 (2011).
- ¹⁵ M. Majumder, K. Ghoshray, A. Ghoshray, B. Bandyopadhyay, B. Pahari, and S. Banerjee, Phys. Rev. B **80**, 212402 (2009).
- ¹⁶ H. Sugawara, K. Ishida, Y. Nakai, H. Yanagi, T. Kamiya, Y. Kamihara, M. Hirano, H. Hosono, J. Phys. Soc. Jpn. **78**, 113705 (2009).
- ¹⁷ M. Majumder, K. Ghoshray, A. Ghoshray, B. Bandyopadhyay, M. Ghosh, Phys. Rev. B **82**, 054422 (2010).
- ¹⁸ C. Krellner, U. Burkhardt, C. Geibel, Physica B **404**, 3206-3209 (2009).
- ¹⁹ Anand Pal, S. S. Mehdi, Mushahid Hussain, Bhasker Gahloti and V. P. S. Awana, arXiv:1105.0971 (2011).
- ²⁰ N. Bloembergen, T. J. Rowland, Acta Mater. **1**, 731 (1953).
- ²¹ C. P. Slichter, *Principles of Magnetic Resonance*, Springer Series in Solid State Sciences I, (Springer-Verlag, 1992).
- ²² M. Belesi, X. Zong, F. Borsa, C. J. Milios, and S. P. Perlepes, Phys. Rev. B **75**, 064414 (2007).
- ²³ W. M. Lomer, Proc. Phys. Soc. **80**, 1380 (1962).
- ²⁴ P. Jeglič, J. -W. G. Bos, A. Zorko, M. Brunelli, K. Koch, H. Rosner, S. Margadonna, and D. Arčon, Phys. Rev. B **79**, 094515 (2009).
- ²⁵ R. Sarkar, A. Jesche, C. Krellner, M. Baenitz, C. Geibel, C. Mazumdar, and A. Poddar, Phys. Rev. B **82**, 054423 (2010).
- ²⁶ G. Prando, P. Carretta, A. Rigamonti, S. Sanna, A. Palenzona, M. Putti, and M. Tropeano, Phys. Rev. B **81**, 100508 (2010).
- ²⁷ K. Ahilan, F. L. Ning, T. Imai, A. S. Sefat, R. Jin, M. A. McGuire, B. C. Sales, and D. Mandrus, Phys. Rev. B **78**, 100501 (2008).
- ²⁸ H. Yamashita, M. Yashima, H. Mukuda, Y. Kitaoka, P. M. Shirage, A. Iyo, Physica C **470**, S375S376 (2010).
- ²⁹ T. Moriya, *Spin Fluctuations in itinerant Electron Magnetism* (Springer-Verlag, New York, 1985).
- ³⁰ T. Moriya, J. Phys. Soc. Jpn. **16**, 23 (1956).
- ³¹ N. Terasaki, H. Mukuda, M. Yashima, Y. Kitaoka, K. Miyazawa, P. M. Shirage, H. Kito, H. Eisaki, and A. Iyo, J. Phys. Soc. Jpn. **78**, 013701, (2009).
- ³² K. Kitagawa, N. Katayama, K. Ohgushi, M. Yoshida, and M. Takigawa, J. Phys. Soc. Jpn. **77**, 114709 (2008).
- ³³ K. Kitagawa, N. Katayama, K. Ohgushi, and M. Takigawa, J. Phys. Soc. Jpn. **78**, 063706 (2009).
- ³⁴ S. Kitagawa, Y. Nakai, T. Iye, K. Ishida, Y. Kamihara, M. Hirano, and H. Hosono, Phys. Rev. B **81**, 212502 (2010).
- ³⁵ F. Ning, K. Ahilan, T. Imai, A. S. Sefat, R. Jin, M. A. McGuire, B. C. Sales, and D. Mandrus, J. Phys. Soc. Jpn. **78**, 013711 (2009).
- ³⁶ F. L. Ning, K. Ahilan, T. Imai, A. S. Sefat, M. A. McGuire, B. C. Sales, D. Mandrus, P. Cheng, B. Shen, and H.-H. Wen, Phys. Rev. Lett. **104**, 037001 (2010).
- ³⁷ K. Ishida, H. Mukuda, Y. Minami, Y. Kitaoka, Z. Q. Mao, H. Fukazawa, Y. Maeno, Phys. Rev. B **64**, 100501(R) (2001).
- ³⁸ T. Moriya, J. Phys. Soc. Jpn. **18**, 516, (1963).
- ³⁹ Albert Narath and H. T. Weaver, Phys. Rev. **175**, 373 (1968).
- ⁴⁰ Chin-Shan Lue and Joseph H. Ross, Jr., Phys. Rev. B **60**, 8533 (1999).
- ⁴¹ M. Hatatani, T. Moriya, J. Phys. Soc. Jpn. **64**, 3434, (1995).
- ⁴² A. Ishigaki, T. Moriya, J. Phys. Soc. Jpn. **67**, 3924, (1998).